Proceedings of the Research Institute of Atmospherics,
Nagoya University, vol. 32(1985) — Technical Note —

REAL TIME SOLAR IMAGE PROCESSOR(RSIP) FOR THE λ 8-cm RADIOHELIOGRAPH AT TOYOKAWA

Masanori Nishio, Yoshio Tsukiji, Shoji Kobayashi
Kiyoto Shibasaki and Shinzo Enome

Abstract

A description is given of the Real-time Solar Image Processor (RSIP). The system is a new back-end processor for the λ 8-cm radioheliograph. By the introduction of the RSIP, the λ 8-cm radioheliograph is converted from the swept-lobe to the multi-correlator type. The RSIP can synthesize one-dimensional and two-dimensional images of the radio sun at a rate of 0.1 s/image and display them in real time. Right and left circular polarizations are obtained by time sharing. The real time phase calibration is made by using redundant antenna combinations. In order to obtain this performance, all correlations necessary for image synthesis and phase calibration are calculated simultaneously, and the Fourier transformation of the correlations and some arrangements to display the images are performed by hardware. The correlators used in the RSIP are of the one-bit type, which are suitable for solar observations because they have a wide dynamic range to the intensity variation.

1. Introduction

The λ 8-cm radioheliograph at Toyokawa has been operating since 1975 (Ishiguro et al., 1975). This system is a multi-element swept-lobe interferometer with a T-shaped array of 3-m diameter paraboloids, consisting of 32+2 elements on the east-west baseline and 16+2 elements on the north-south baseline. The baseline length is 437 m in the east-west direction and 217 m in the north-south direction, and the fundamental antenna spacing is 6.88 m. This system gives two-dimensional brightness distributions of the radio sun as well as one-dimensional east-west and north-south distributions with higher spatial resolution than two-dimensional observation.

In the original system the solar radio maps were obtained by sweeping the beam of the interferometer across the sun, thereby obtaining sequential amplitude data corresponding to each position on the sun. In this case, integration time cannot be as long as the time required to obtain a map, since the beam focuses on a particular picture cell to the exclusion of others. For example, the integration time must be less than 1/1024 of the time required to obtain a map of 32×32 picture elements. If we obtain a map with a time resolution of 0.1 s, the integration time for each picture cell comes out to be less than 0.1 ms and the sensitivity is not sufficient for a precise map. Therefore, the original system is suitable for the observation of quasi-stationary structures, such as the coronal holes (Shibasaki et al., 1978) or the large scale coronal structure around the equator (Ishiguro et al., 1980). In order to observe the radio bursts of fast time variation, we decided to improve the time resolution of the λ 8-cm radioheliograph. There are two ways to do this without sacrificing sensitivity. One way is to use the multi-beam type system which consists of the Butler matrix and signal detectors, and the other is to use the multi-correlator type system which consists of correlators and a Fourier transformer. The former option requires a relatively simple construction, but the phase adjustment of the Butler matrix is very complex. Therefore, the latter option was adopted in our new system. As the first step in converting the λ 8-cm radioheliograph to the multi-correlator type system, the waveguide branching network of the original system was replaced by low-noise, phase-stable, front-end receivers and low-loss, phase stable, coaxial cables, which were installed at each element antenna (Nishio et al., 1984). At the same time, a design study on the correlator system was done in conjunction with this improvement (Nishio et al, 1982).

In 1983, a project to adapt the Real-time Solar Image Processor (RSIP) to the present back-end receiver was begun spanning both FY

1983 and 1984. The RSIP consists of six components: a third IF, A/D converter, correlator, Fourier transformer, data storage system and image display. Presently, the first three components have been installed and experiments to check their performance are in progress. In this report, an outline of the RSIP is described.

2. Design principle and performance

The RSIP is designed to satisfy the following two requirements;

(1) to improve the time resolution of the λ 8-cm radioheliograph up to 0.1 s/image without sacrificing sensitivity.

(2) to produce solar images in real time.

In order to improve time resolution, all correlations necessary to construct an image and for phase calibration are measured in parallel. As a result, 1308 correlations are obtained simultaneously. In order to produce the image in real time, the Fourier transformation which is used to obtain solar images from the correlation data and some of the arrangements necessary to display the images are performed by hardware. In the RSIP, correlation data are recorded at the rate of 0.1 seconds an image and the image data are displayed on a graphic terminal at the rate of 10 seconds an image.

The frequency conversion of the input signal to the baseband signal is performed by the double sideband mixer because it is possible to perform delay-tracking and phase-tracking independently (O'Sullivan, 1976). In the double sideband system, all four correlations, i.e. the cosine×cosine, cosine×sine, sine×cosine and sine×sine correlations, must be measured to each pair of the input signals in order to obtain sensitivity equal to that of the single sideband system. Therefore the correlator number is twice that of the single sideband system. The correlators used in the RSIP are of the one-bit type. Because they are relatively insensitive to the amplitude variation of the input signals and have a wide dynamic range to the amplitude variation, one-bit type correlators are suitable for solar observations where large amplitude variations occur as compared with that of cosmic sources. One-bit correlation data can be converted to multi-bit correlation data by Van Vleck's correction (Van Vleck and Middleton, 1966).

The expected performance of the radioheliograph after this improvement is listed in table 1. In the original swept-lobe type

system it takes over 40 s to obtain a two-dimensional image and over 10 s to obtain a one-dimensional image. Therefore the time resolution is improved 400 times for the two-dimensional image and 100 times for the one-dimensional image. The minimum detectable flux density is obtained from following equation;

$$\Delta S_{min} = \frac{10\ M\ k\ (T_o + T_R)}{A_e\ (N\ B\ \tau)^{1/2}} \quad W\ m^{-2}\ Hz^{-1}$$

where M is a degradation factor depending on both the interferometer detection type and the method of time sharing; k is the Boltzmann constant; T_o and T_R are the antenna temperature(K) and the receiver

Table 1. Performance of the λ 8-cm radioheliograph with the RSIP

Observation frequency	3748.5 MHz (=center frequency)	
Bandwidth	10 MHz	#1
Observation time	meridian transit time ± 3 hours	
Field of view	40 arc min×40 arc min	
Observation mode	two-dimension	
(parallel obs.)	east-west one-dimension	
	north-south one-dimension	
	(phase error measurement)	
Spatial resolution	2.5×2.5 arc min (two dimension)	
	38 arc sec (EW one dimension)	
	1.25 arc min (NS one dimension)	
Max. time resolution	0.1 sec/2 maps	
	(R and L polarization maps)	#2
Minimum detectable flux density	(integration time=0.05 sec)	
	0.08 s.f.u. (two dimension)	#3
	0.2 s.f.u. (EW one dimension)	
	0.3 s.f.u. (NS one dimension)	
Polarization	R and L circular polarizations	
	(time sharing by Polarization switches)	
Display speed	real time(10 s/image)	

#1 usually 2 MHz in the original system.
#2 greater than 40 s/image (two-dimension)
and 10 s/image (one-dimension) in the original system.
#3 1 s.f.u.(Solar Flux Unit)=10^{-22} W m^{-2} Hz^{-1}

noise temperature(K), respectively; A_e is the effective collecting area of the element antenna in square meters; N is the number of observed Fourier components; B is the bandwidth in heltz; and τ is the integration time in seconds. In the λ 8-cm radioheliograph, $T_R \simeq 1000$ K and $A_e \simeq 4.2$ m^2. When solar activity is very low, $T_O \simeq 1000$ K. M is $2\sqrt{2}$ for the original system because RH and LH circular polarization are measured by time sharing and only the real components of signals are measured. The minimum detectable flux density of the two-dimensional mode, the east-west one-dimensional compound mode, and the north-south one-dimensional compound mode are 0.082, 0.23 and 0.33 s.f.u., respectively. In the improved system, The one-bit correlators are used by two-times oversampling and the degradation factor of the signal-to-noise ratio of the one-bit correlation compared with that of the analogue correlation is 1.35 (Bowers and Klingler, 1974). RH and LH circular polarization components are measured by time sharing and the real and the imaginary components of correlations are measured simultaneously. Therefore, M is 2.7 and the minimum detectable flux density is nearly equal to that of the original system.

3. Outline of the system

The block diagram of the λ 8-cm radioheliograph with the RSIP is shown in figure 1, where the RSIP is enclosed by a dash-dotted line. The RSIP consists of six components: a third IF, A/D converter, correlator, Fourier transformer, data storage system and image display. The third IF is installed near the phase center of the antenna array together with the second IF of the radioheliograph system, and other parts are placed in the observation building about 200 m apart from the phase center.

The outputs of the second IF of the radioheliograph system are fed into the RSIP. At the third IF, input signals are amplified and frequency-converted to base-band signals. The output signals of the third IF are transmitted to the A/D converters through coaxial cables. In the A/D converters, the base-band signals are sampled and digitized to one-bit signals. The relative propagation delays among the received signals are equalized here. These one-bit digital signals are cross-correlated to obtain the spatial frequency components of two-dimensional and one-dimensional solar images. The solar images are

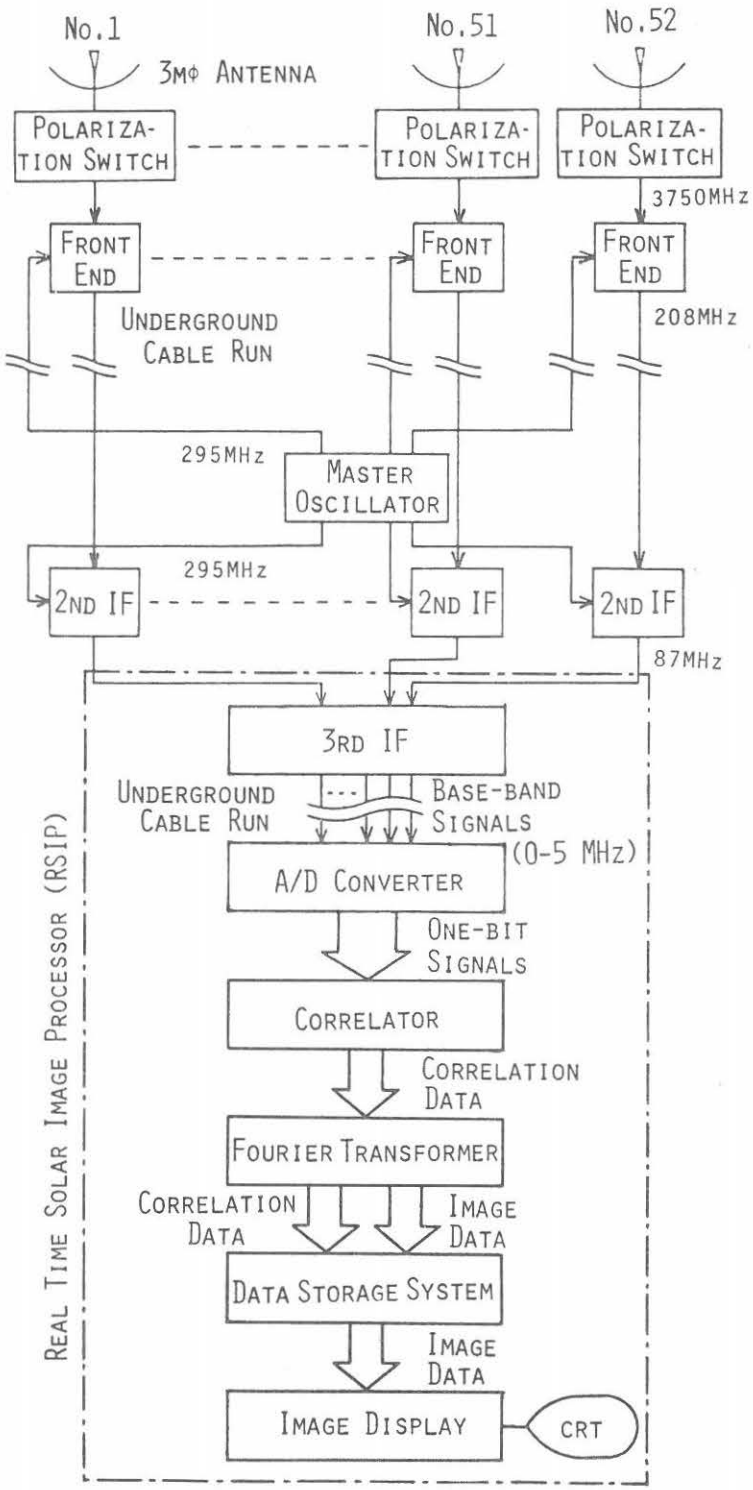

Fig. 1. Block diagram of the λ 8-cm radioheliograph with the RSIP.

obtained by the Fourier transformation of the correlators' output data. These images are displayed on a graphic terminal in order to monitor solar activity in real time. On the other hand, correlation data are stored in the data storage system for off-line analysis.

3.1 Third IF

This component consists of 52 modules corresponding to the number of input channels. One module is shown in figure 2. Each module consists of an IF amplifier, a remote-controllable PIN attenuator, two DSB mixers and two video amplifiers. Each input signal is converted to two base-band signals. The signals are orthogonal to each other in order to obtain the real and the imaginary halves of the spatial frequency components simultaneously. Therefore the output channel number is twice that of the input channel, or 104. The DSB mixers are used and the higher cut-off frequency of the base-band signals is 5 MHz. The bandwidth of the received signals is 10 MHz. The total gain here is 40 dB, and an output signal level of about -7 dBm can be obtained even when solar activity is very low, corresponding to 0.1 V rms for 50-ohm output impedance.

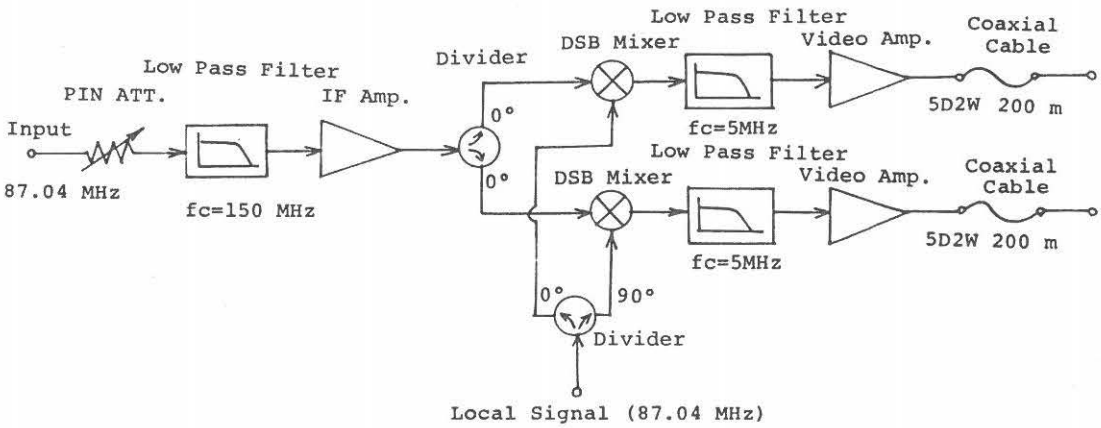

Fig. 2. A module of the third IF.

3.2 A/D Converter

The A/D converter consists of three units; a fast one-bit sampler unit, a delay-tracking unit and a signal intensity monitor.

The fast one-bit sampler unit functions to sample the analogue input signals with the higher cut-off frequency of 5 MHz and convert

them into one-bit digital signals. The input signals of 104 channels are sampled and digitized simultaneously. The sampling frequency is twice the Nyquest sampling rate, or 20 MHz. By doubling the sampling the degradation factor can be decreased by 14 % compared with regular sampling (Bowers and Klingler, 1974). A level regulation circuit is attached to each comparator, which compensates for the drift of the comparator's threshold level (O'Sullivan, 1980).

The delay-tracking unit functions to compensate for the differences in the signal arrival time between antennas, consisting of 104 modules corresponding to the number of signal channels. Each module is composed of two types of digital delay lines, fine and coarse, and a resampling circuit as shown in figure 3. The fine delay line has a delay step of 10 ns and a maximum delay time of 40 ns, while the coarse delay line has a delay step of 50 ns and a maximum delay time of 1050 ns. The former is connected to the sampling clock input of the sampler and shifts the timing of sampling. The latter is attached to the output of the sampler and gives the delay to the sampled data. By the combination of these delay lines, a delay step of 10 ns and a maximum delay time of 1090 ns (109 steps) are obtained without using the 100-MHz sampling clock. The output of the coarse delay line was resampled by the resampling circuit, in which the clock is synchronized to the clock of the correlator.

The signal intensity monitor functions to obtain the signal intensity received by each channel. The signal intensity data are

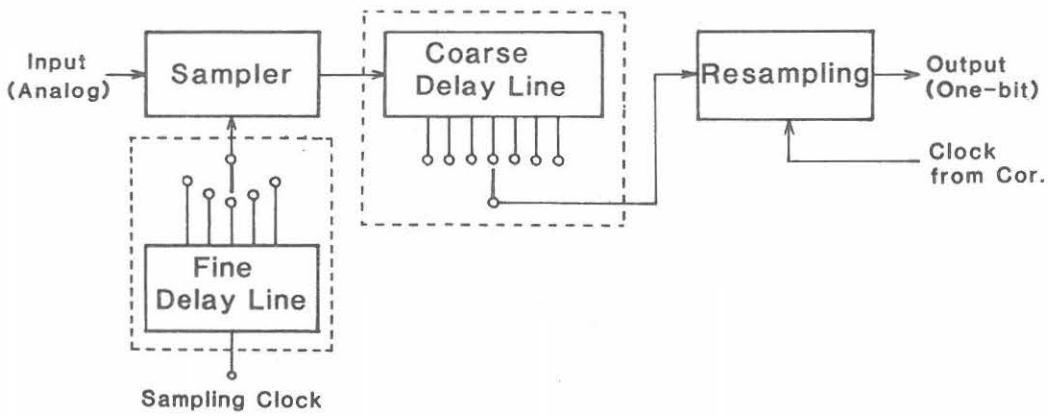

Fig. 3. Schematic diagram of the hybrid delay line.

digitized by a 12-bit A/D converter circuit and transmitted to the data storage system so that amplitude information from the correlation data can be recovered.

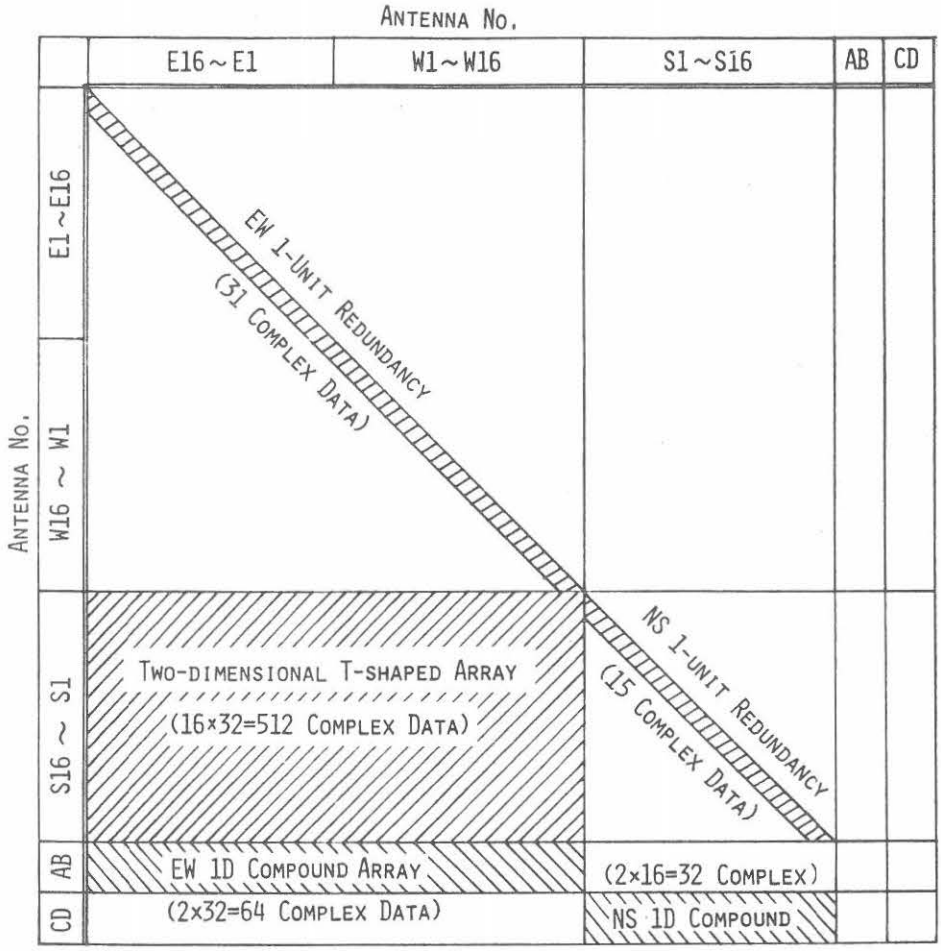

Used antenna combinations are shown by ▨ or ▨.

The number of pre-scalers:

Two-dimension	512×4=2048
EW one-dimension	64×4= 256
NS one-dimension	32×4= 128
EW 1-unit redundancy	31×4= 124
NS 1-unit redundancy	15×4= 60
Total	2616

Fig. 4. Antenna combinations used in the RSIP.

3.3 Correlator

In the RSIP, 654 complex correlations are calculated simultaneously. Figure 4 is the antenna combination diagram used in this system. The correlation data obtained are divided to four segments: two-dimensional correlation data, east-west one-dimensional correlation data, north-south one-dimensional correlation data and the correlation data for phase calibration.

This component consists of 2616 pre-scalers and an integration unit as shown in figure 5. Each pre-scaler is made by an exclusive OR circuit and a 16-bit binary counter. In these circuits, one-bit

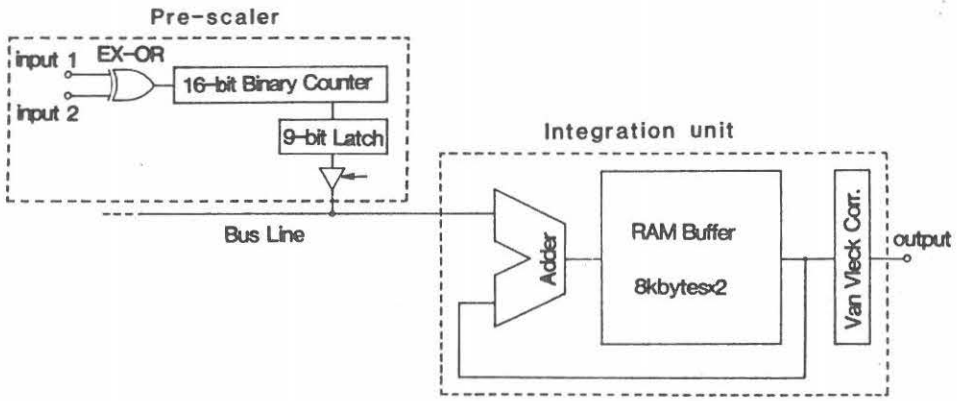

Fig. 5. A pre-scaler module and the integration unit.

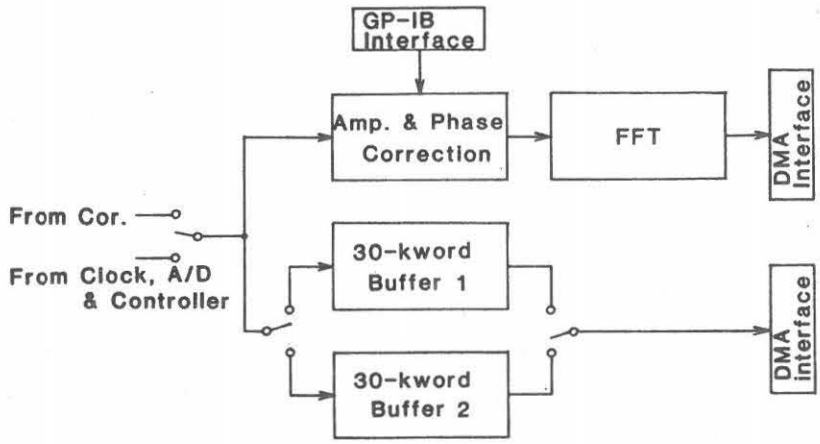

Fig. 6. The Fourier transformer.

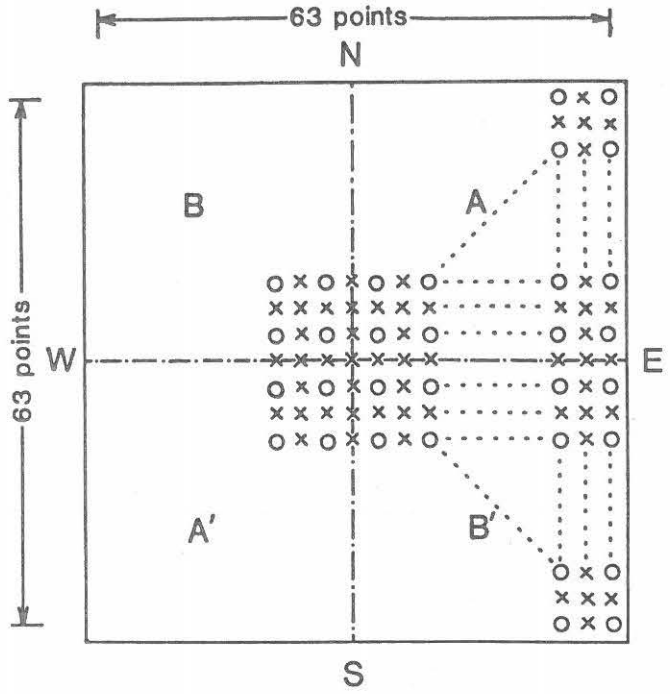

(a)

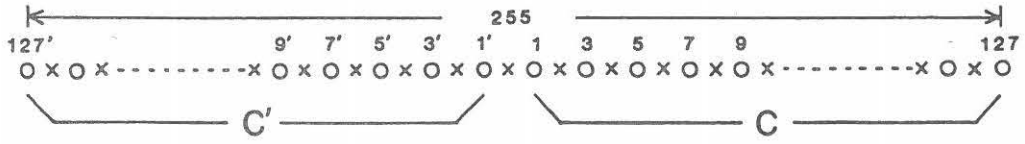

(b)

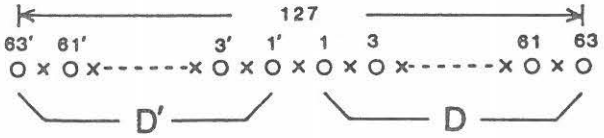

(c)

Fig. 7. Sampled points on the spatial frequency domain. Odd components are sampled data and even components are zero.
(a) Two-dimensional data.
(b) East-west one-dimensional data.
(c) North-south one-dimensional data.

correlation data with an integration time of about 3 ms are produced. The switching rate of polarization is 60 Hz and correlation data are obtained twice every switching interval. These data are read out sequentially through the bus-lines and transmitted to the integration unit. The integration unit consists of a 12-bit adder, two RAM buffers and a Van Vleck correction circuit. The output data of the pre-scalers are integrated for 0.1 s in this unit. The Van Vleck correction is performed by Read Only Memorys (ROM).

3.4 Fourier Transformer

This component consists of an amplitude and phase correction circuit, a Fast Fourier Transformation (FFT) circuit and two 30-kword buffers as shown in figure 6. Amplitude and phase errors included in the correlation data are removed in the amplitude and phase correction circuit. Corrected data are converted to image data by the FFT circuit and transmitted to the data storage system. The correlation data fed to the 30-kword buffers are directly transmitted to the data storage system. The Fourier transformation is performed by FFT hardware. The amplitude and phase errors are corrected by hardware.

Figure 7 shows the sampled points in the spatial frequency domain. In the T-shaped array configuration, spatial frequency components are sampled at Cartesian grid points, which is convenient to perform the Fast Fourier Transformation in real time. Two-dimensional, east-west one-dimensional and north-south one-dimensional data consist of 64×64, 256 and 128 grid points respectively, where only odd harmonics have non-zero values and even harmonics are set to zero.

3.5 Data Storage System

The data storage system consists of a mini-computer with two 167-Mbyte magnetic disk units and a magnetic tape unit as shown in figure 8. The Fourier transformer and the data storage system are connected with two DMA channels and a GP-IB channel. These DMA channels are used for the transmission of image and correlation data. The data used for amplitude and phase correction in the Fourier transformer are sent through the GP-IB channel. The transmission rate of the image data is about 0.5 kbytes/s which corresponds to 10 s a set of image, where a set of image consists of a two-dimensional intensity image, a two-dimensional polarization degree image, a east-west one-dimensional intensity image, a east-west one-dimensional polarization degree

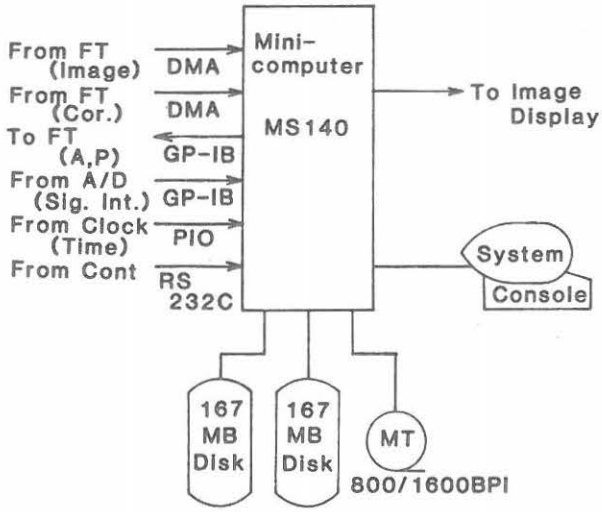

Fig. 8. The data storage system.

image, a north-south one-dimensional intensity image and a north-south one-dimensional polarization degree image. The total amount of image data is 11 Mbytes for 6 hours. Correlation data is obtained at the rate of 60 Kbytes/s and the total amount of data is 1.3 Gbytes for 6 hours. The amount of correlation data will be reduced up to one reel of magnetic tape a day by adjusting the rate of data storage in accordance with the solar activity.

3.6 Image Display

In this component, the coordinates of the two-dimensional images are rotated to bring the north pole to the top of the map and the picture elements are rearranged on fixed grid points. These processes are performed by hardware and the images are displayed at a rate of 10 seconds/image along with one-dimensional images.

The image display is closely connected with the data storage system. The image data and the control commands are transmitted from the data storage system.

4. Preliminary results of test operations

Figure 9 and 10 are the results of test operations using the 3rd IF, the A/D converter and the correlator. The digital output data of the pre-scaler modules of the correlator were recorded on a chart-

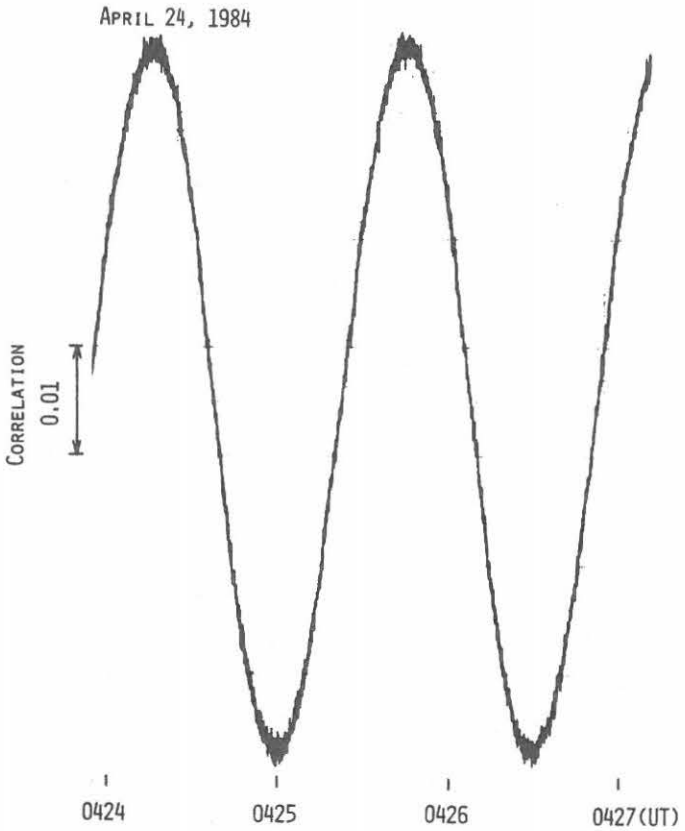

Fig. 9. Fringe pattern for the baseline of twice the unit antenna spacing.

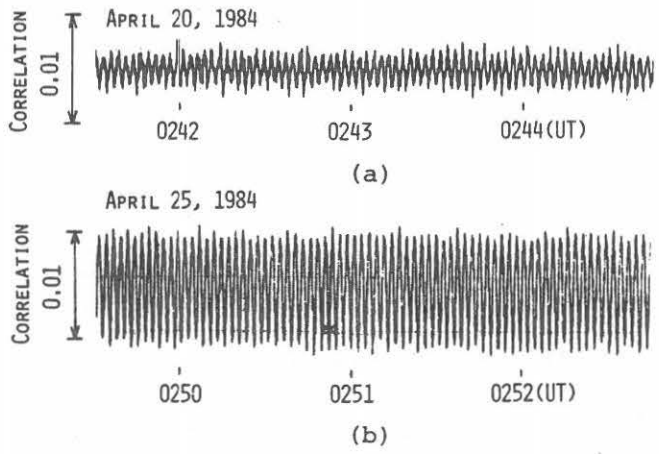

Fig. 10. Fringe patterns for the maximum east-west baseline.
(a) non-burst period.
(b) during the burst.

recorder through a Van Vleck correction circuit and a digital-to-analogue converter circuit. In these figures, the ordinate is the output voltage and the abscissa is the time. In the one-bit correlator, the output voltage has no amplitude information from the input signals. Therefore, the scale of the ordinate is normalized by the maximum value. The integration time in the pre-scaler modules was 6.6 ms. Phase tracking was not performed in these test operations, so sinusoidal fringe patterns due to the earth rotation were obtained. Figure 9 is a fringe pattern to the baseline of twice the unit antenna spacing. In this figure, the fringe amplitude is about 0.065 and the fluctuation level of the output voltage is less than 0.002 in rms, resulting in a signal-to-noise ratio of greater than 15 dB. During normal operation, the integration time of the RSIP is 53 ms and a signal-to-noise ratio greater than 24 dB is expected. During the test operation, the system noise temperature was about 3000 K. From these values, a minimum detectable temperature of less than 6 K is obtained. Figure 10 cosists of fringe patterns obtained for the maximum east-west baseline of the λ 8-cm radioheliograph. In the non-burst period, the extended component is dominant in the solar radio image, and the fringe amplitude for the long baselines is very low compared with that for the short baselines. Figure 10(a) is the data from the non-burst period and figure 10(b) is that during the burst. In both figures, similar fringe patterns can be seen. Therefore, it is confirmed that clear solar images with a time resolution of 0.1 s will be obtained even during a non-burst period.

Acknowledgements

We wish to express our thanks to Dr. A. Bos for his useful suggestion in system design. We appreciate very much Messrs. T. Takayanagi, C. Torii, N. Yoshimi and S. Takata for their supports in constructing this system.

References

Bowers, F. K., and Klingler, R. J.: Quantization Noise of Correlation Spectrometers, Astron. Astrophys. Suppl., 15, 373-380 (1974).

Ishiguro, M., Enome, S., Shibasaki, K., and Tanaka, H.: Observation of the Quiet Sun during the Solar Minimum (Cycle 20-21) with the Toyokawa λ 8-cm Radioheliograph, Publ. Astron. Soc. Japan, **32**, 533-541 (1980).

Ishiguro, M., Tanaka, H., Enome, S., Torii, C., Tsukiji, Y., Kobayashi, S., and Yoshimi, N.: 8-cm Radioheliograph, Proc. Res. Inst. Atmospherics, Nagoya Univ., **22**, 1-25 (1975).

Nishio, M., Tsukiji, Y., Enome, S., Shibasaki, K., and Morita, K.-I.: A Design Study and some Experiments of Digital Correlator Backend for λ 8-cm Radioheliograph at Toyokawa, Proc. Res. Inst. Atmospherics, Nagoya Univ., **29**, 47-60 (1982).

Nishio, M., Torii, C., Enome, S., Shibasaki, K., Tsukiji, Y., Kobayashi, S., Yoshimi, N., Takata, S., Takayanagi, T., and Ishiguro, M.: The Improved λ 8-cm Radioheliograph at Toyokawa, Publ. Astron. Soc. Japan, **36**, 371-381 (1984).

O'Sullivan, J. D.: Outline of a Proposed Broadband Backend System for the SRT, Netherlands Fundation for Radio Astronomy-Internal Technical Report **146**, 1-61 (1976).

O'Sullivan, J. D.: Level Regulation in the DCB Analogue to Digital Converters, Netherlands Fundation for Radio Astronomy-Note **329**, 1-13 (1980).

Shibasaki, K., Ishiguro, M., Enome, S., and Tanaka, H.: A Coronal Hole Observed with a λ 8-cm Radioheliograph, Publ. Astron. Soc. Japan, **30**, 589-600 (1978).

Van Vleck, J. H., and Middleton, D.: The Spectrum of Clipped Noise, Proc. IEEE, **54**, 2-19 (1966).